Inorg. Chem. **2004**, *43*, 2624–2635

Synthesis and Characterization of Zinc Sensors Based on a Monosubstituted Fluorescein Platform

Elizabeth M. Nolan, Shawn C. Burdette, Jessica H. Harvey, Scott A. Hilderbrand, and Stephen J. Lippard*

Department of Chemistry, Massachusetts Institute of Technology, Cambridge, Massachusetts 02139

Received October 6, 2003

The synthesis of a new fluorescein carboxaldehyde asymmetrically substituted on the xanthene (top) ring is reported. This molecule is a key precursor for two of three monofunctionally derivatized fluorescein-based Zn(II) sensors presented in this work. Detailed preparative routes to, and photophysical characterization of, these sensors are described. The sensors are based on the previously reported ZP4 motif (Burdette, S. C.; Frederickson, C. J.; Bu, W.; Lippard, S. J. *J. Am. Chem. Soc.* **2003**, *125*, 1778–1787) and incorporate a di(2-picolyl)amine-containing aniline-derivatized ligand framework. By varying the nature of the substituent (X) para to the aniline nitrogen atom, which is responsible for PET quenching of the unbound ZP dye, we investigated the extent to which such electronic tuning might improve the fluorescent properties of asymmetrical ZP sensors. Although a comparison of probes with X = H, F, Cl, OMe reveals that the photophysical behavior of these dyes is not readily predictable, our methodology illustrates the ease with which aniline-based ligands may be linked to fluorescein dyes.

Introduction

The role of zinc in neurobiology is a topic of substantial current interest.[1−3] Although Zn(II) homeostasis is tightly regulated by a number of homologous Zn(II) transporter proteins (ZnTs)[4,5] and metallothionens,[6−8] pools of loosely bound or "free" Zn(II) occur in the mossy fiber terminals of the hippocampus, the center of learning and memory in the brain.[2,9,10] Zinc concentrations of ∼0.3 mM are achieved in vesicles in the presynaptic terminals of these cells. Release of Zn(II) from these vesicles has been implicated in neurological processes including long-term potentiation[11] and neurotransmission.[12−15] Uncontrolled Zn(II) release from the mossy fiber terminals after traumatic brain injury, stroke, or seizure results in neuronal death.[16,17] The disruption of Zn(II) homeostasis may also contribute to the pathology of Alzheimer's disease and other neurological disorders.[15,18] Despite these implications, the functional significance of Zn(II) in neurobiology remains unclear.[19−22]

In order to elucidate the role of Zn(II) in such events, detection methods that exhibit selectivity and sensitivity for Zn(II) and are also suitable for use in biological fluids are required.[23−25] Fluorescence sensors are excellent tools for studying biological processes and are particularly well suited for optical detection of Zn(II), a d^{10} metal ion that cannot

* To whom correspondence should be addressed. E-mail: lippard@lippard.mit.edu.

(1) Vallee, B. L.; Falchuk, K. H. *Physiol. Rev.* **1993**, *73*, 79−118.
(2) Frederickson, C. J.; Moncrieff, D. W. *Biol. Signals* **1994**, *3*, 127−139.
(3) Takeda, A. *BioMetals* **2001**, *14*, 343−351.
(4) Cole, T. B.; Wenzel, H. J.; Kafer, K. E.; Schwartzkroin, P. A.; Palmiter, R. D. *Proc. Natl. Acad. Sci. U.S.A.* **1999**, *96*, 1716−1721.
(5) Valente, T.; Auladell, C. *Mol. Cell. Neurosci.* **2002**, *21*, 189−204.
(6) Vasak, M.; Hasler, D. W. *Curr. Opin. Chem. Biol.* **2000**, *4*, 177−183.
(7) Jacob, C.; Maret, W.; Vallee, B. L. *Proc. Natl. Acad. Sci. U.S.A.* **1998**, *95*, 3489−3494.
(8) Ebadi, M.; Iversen, P. L.; Hao, R.; Cerutis, D. R.; Rojas, P.; Happe, H. K.; Murrin, L. C.; Pfeiffer, R. F. *Neurochem. Int.* **1995**, *27*, 1−22.
(9) Frederickson, C. J. *Int. Rev. Neurobiol.* **1989**, *31*, 145−238.
(10) Budde, T.; Minta, A.; White, J. A.; Kay, A. R. *Neuroscience* **1997**, *79*, 347−358.
(11) Li, Y.; Hough, J. H.; Frederickson, C. J.; Sarvey, J. M. *Neuroscience* **2001**, *21*, 8015−8025.
(12) Huang, E. P. *Proc. Natl. Acad. Sci. U.S.A.* **1997**, *94*, 13386−13387.
(13) Howell, G. A.; Welch, M. G.; Frederickson, C. J. *Nature* **1984**, *308*, 735−738.
(14) Frederickson, C. J.; Bush, A. I. *BioMetals* **2001**, *14*, 353−366.
(15) Cuajungco, M. P.; Lees, G. J. *Neurobiol. Dis.* **1997**, *4*, 137−169.
(16) Suh, S. W.; Chen, J. W.; Motamedi, M.; Bell, B.; Listiak, K.; Pons, N. F.; Danscher, G.; Frederickson, C. J. *Brain Res.* **2000**, *852*, 268−273.
(17) Choi, D. W.; Koh, J. Y. *Annu. Rev. Neurosci.* **1998**, *21*, 347−375.
(18) Bush, A. I. *Curr. Opin. Chem. Biol.* **2000**, *4*, 184−191.
(19) Cole, T. B.; Martyanova, A.; Palmiter, R. D. *Brain Res.* **2001**, *891*, 253−265.
(20) Lee, J.-Y.; Park, J.; Kim, Y.-H.; Kim, D. H.; Kim, C. G.; Koh, J.-Y. *Exp. Neurol.* **2000**, *161*, 433−441.
(21) Lee, J.-Y.; Cole, T. B.; Palmiter, R. D.; Koh, J.-Y. *Neuroscience* **2000**, *20:RC79*, 1−5.
(22) Kay, A. R. *J. Neurosci.* **2003**, *23*, 6847−6855.

10.1021/ic035158+ CCC: $27.50
Published on Web 03/16/2004

readily be probed by using conventional absorption spectroscopy. Small synthetic molecules that combine a Zn(II) binding unit with a fluorophore and change either fluorescence intensity or wavelength upon Zn(II) coordination provide one powerful approach. Accordingly, several intensity-based small molecule fluorescent Zn(II) sensors have been studied and include aryl sulfonamides,[26−32] probes incorporating macrocyclic Zn(II) binding units,[28,33−35] members of the ZnAF family,[36,37] and modified calcium sensors.[38,39] Sensing strategies based on proteins[40−42] and peptides,[43−47] and small molecule ratiometric Zn(II) sensors, have also been reported.[48−51]

Motivated to study the enigmatic role of Zn(II) in neurobiology, our laboratory has devised the Zinpyr (ZP) family of Zn(II) probes (Figure 1).[52−55] These sensors give a positive fluorescence response upon Zn(II) or Cd(II) coordination. The first-generation ZP probes, ZP1 (**1**) and ZP2 (**2**), exhibit ∼3 to ∼6-fold fluorescence enhancement upon addition of 1 equiv of Zn(II).[52,53] They have relatively high background fluorescence ($\phi = 0.32$, ZP1; 0.25, ZP2) and can form dinuclear Zn(II) complexes owing to the two di(2-picolyl)amine (DPA) moieties installed on the 4′ and 5′ positions of the xanthenone ring. ZP3 (**3**), the most recent symmetrical ZP probe, exhibits improved dynamic range.[55] In an effort to lower the background fluorescence of the free ZP dyes and to obtain mononuclear Zn(II) complexes, the second-generation Zn(II) sensor ZP4 (**4**) was created (Figure 1).[54] This sensor contains an aniline-derived DPA-derivatized ligand framework linked to an unsymmetrical functionalized fluorescein platform. It exhibits lower background fluorescence ($\phi = 0.06$) than the first-generation probes attributed to a lowering of the pK_a values of the nitrogen atoms responsible for photoinduced electron transfer (PET) quenching[56,57] of the free ZP dyes.[54,55] A lower pK_a value, observed for ZP4 relative to ZP1 and ZP2, corresponds to more efficient PET quenching and a smaller quantum yield for the unbound ZP dye.

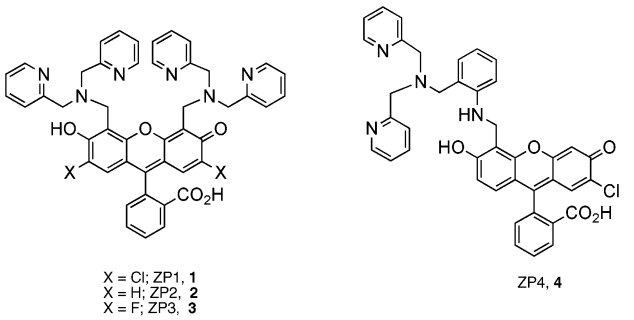

Figure 1. Members of the Zinpyr (ZP) family of fluorescent Zn(II) sensors.

In the present work, we studied the effect of electronic variation on the fluorescence properties of unsymmetrical ZP4-like sensors. We reasoned that, by altering the electronic properties of the ligand, we might further tune the pK_a of the nitrogen atom responsible for PET quenching and control the fluorescence properties of the sensor. Toward this end, we synthesized three new ZP sensors by varying the electron donating and withdrawing nature of the substituent para to the aniline nitrogen atom (X = F, Cl, OMe). Photophysical characterization of these compounds reveals both expected and unanticipated behavior.

Experimental Section

Reagents. Ethyl acetate, dimethylformamide, and pyridine were dried over 3 Å molecular sieves. Chlorobenzene and 1,2-dichlo-

(23) Burdette, S. C.; Lippard, S. J. *Proc. Natl. Acad. Sci. U.S.A.* **2003**, *100*, 3605−3610.
(24) Kimura, E.; Koike, T. *Chem. Soc. Rev.* **1998**, *27*, 179−184.
(25) Burdette, S. C.; Lippard, S. J. *Coord. Chem. Rev.* **2001**, *216−217*, 333−361.
(26) Frederickson, C. J.; Kasarskis, E. J.; Ringo, D.; Frederickson, R. E. *J. Neurosci. Methods* **1987**, *20*, 91−103.
(27) Kimber, M. C.; Mahadevan, I. B.; Lincoln, S. F.; Ward, A. D.; Tiekink, E. R. T. *J. Org. Chem.* **2000**, *65*, 8204−8209.
(28) Xue, G.; Bradshaw, J. S.; Dalley, N. K.; Savage, P. B.; Izatt, R. M.; Prodi, L.; Montalti, M.; Zaccheroni, N. *Tetrahedron* **2002**, *58*, 4809−4815.
(29) Hendrickson, K. M.; Rodopoulos, T.; Pittet, P.-A.; Mahadevan, I.; Lincoln, S. F.; Ward, A. D.; Kurucsev, T.; Duckworth, P. A.; Forbes, I. J.; Zalewski, P. D.; Betts, W. H. *J. Chem. Soc., Dalton Trans.* **1997**, 3879−3882.
(30) Nasir, M. S.; Fahrni, C. J.; Suhy, D. A.; Kolodsick, K. J.; Singer, C. P.; O'Halloran, T. V. *J. Biol. Inorg. Chem.* **1999**, *4*, 775−783.
(31) Kim, T. W.; Park, J.; Hong, J.-I. *J. Chem. Soc., Perkin. Trans. 2* **2002**, 923−927.
(32) Fahrni, C. J.; O'Halloran, T. V. *J. Am. Chem. Soc.* **1999**, *121*, 11448−11458.
(33) Hirano, T.; Kazuya, K.; Urano, Y.; Higuchi, T.; Nagano, T. *Angew. Chem., Int. Ed.* **2000**, *39*, 1052−1053.
(34) Koike, T.; Watanabe, T.; Aoki, S.; Kimura, E.; Shiro, M. *J. Am. Chem. Soc.* **1996**, *118*, 12696−12703.
(35) Aoki, S.; Kaido, S.; Fujioka, H.; Kimura, E. *Inorg. Chem.* **2003**, *42*, 1023−1030.
(36) Hirano, T.; Kikuchi, K.; Urano, Y.; Higuchi, T.; Nagano, T. *J. Am. Chem. Soc.* **2000**, *122*, 12399−12400.
(37) Hirano, T.; Kikuchi, K.; Urano, Y.; Nagano, T. *J. Am. Chem. Soc.* **2002**, *124*, 6555−6562.
(38) Gee, K. R.; Zhou, Z.-L.; Ton-That, D.; Sensi, S. L.; Weiss, J. H. *Cell Calcium* **2002**, *31*, 245−251.
(39) Gee, K. R.; Zhou, Z. L.; Qian, W.-J.; Kennedy, R. *J. Am. Chem. Soc.* **2002**, *124*, 776−778.
(40) Thompson, R. B.; Cramer, M. L.; Bozym, R.; Fierke, C. A. *J. Biomed. Opt.* **2002**, *7*, 555−560.
(41) Thompson, R. B.; Whetshell, W. O.; Maliwal, B. P.; Fierke, C. A.; Frederickson, C. J. *J. Neuro. Met.* **2000**, *96*, 35−45.
(42) Elbaum, D.; Nair, S. K.; Patchan, M. W.; Thompson, R. B.; Chirstianson, D. W. *J. Am. Chem. Soc.* **1996**, *118*, 8381−8387.
(43) Walkup, G. K.; Imperiali, B. *J. Org. Chem.* **1998**, *63*, 6727−6731.
(44) Walkup, G. K.; Imperiali, B. *J. Am. Chem. Soc.* **1996**, *118*, 3053−3054.
(45) Jotterand, M.; Pearce, D. A.; Imperiali, B. *J. Org. Chem.* **2001**, *66*, 3224−3228.
(46) Godwin, H. A.; Berg, J. M. *J. Am. Chem. Soc.* **1996**, *118*, 6514−6515.
(47) Shults, M. D.; Pearce, D. A.; Imperiali, B. *J. Am. Chem. Soc.* **2003**, *125*, 10591−10597.
(48) Maruyama, S.; Kikuchi, K.; Hirano, T.; Urano, Y.; Nagano, T. *J. Am. Chem. Soc.* **2002**, *124*, 10650−10651.
(49) Woodroofe, C. C.; Lippard, S. J. *J. Am. Chem. Soc.* **2003**, *125*, 11458−11459.
(50) Taki, M.; Wolford, J. L.; O'Halloran, T. V. *J. Am. Chem. Soc.* **2004**, *126*, 712−713.
(51) Chang, C. J.; Jaworski, J.; Nolan, E. M.; Sheng, M.; Lippard, S. J. *Proc. Natl. Acad. Sci. U.S.A.* **2004**, *101*, 1129−1134.
(52) Walkup, G. K.; Burdette, S. C.; Lippard, S. J.; Tsien, R. Y. *J. Am. Chem. Soc.* **2000**, *122*, 5644−5645.
(53) Burdette, S. C.; Walkup, G. K.; Spingler, B.; Tsien, R. Y.; Lippard, S. J. *J. Am. Chem. Soc.* **2001**, *123*, 7831−7841.
(54) Burdette, S. C.; Frederickson, C. J.; Bu, W.; Lippard, S. J. *J. Am. Chem. Soc.* **2003**, *125*, 1778−1787.
(55) Chang, C. J.; Nolan, E. M.; Jaworski, J.; Burdette, S. C.; Sheng, M.; Lippard, S. J. *Chem. Biol.* **2004**, *11*, 203−210.
(56) Czarnik, A. W. *Acc. Chem. Res.* **1994**, *27*, 302−308.
(57) de Silva, A. P.; Gunaratne, Q. N.; Gunniaugsson, T.; Huxley, A. J.; McCoy, C. P.; Rademacher, J. T.; Rice, T. E. *Chem. Rev.* **1997**, *97*, 1515−1566.

roethane (DCE) were distilled from CaH_2 under nitrogen and stored over 3 Å molecular sieves. Acetonitrile was either distilled over CaH_2 under nitrogen or was saturated with Ar and dried by passing through an activated Al_2O_3 column. DMSO was vacuum distilled from CaH_2 immediately before use or purchased in its anhydrous form. 7′-Chloro-4′-methylfluorescein, **13**, and 7′-chloro-4′-bromomethylfluorescein di-*tert*-butyldimethylsilyl ether, **22**, were synthesized as previously described.[54] All other reagents were used as received.

Methods. Silica gel-60 (230−400 mesh), Brockman I activated basic aluminum oxide (150 mesh), and octadecyl-functionalized silica gel (reverse phase) were used as the solid phases for column chromatography. Thin-layer chromatography (TLC) was performed by using Merck F254 silica gel-60 plates, Merck F254 aluminum oxide-60 plates, or octadecyl-functionalized silica gel (RP18) plates. TLC plates were viewed with UV light or after developing with ninhydrin stain. NMR spectra were collected using either a Varian 300 MHz, a Varian 500 MHz, or a Bruker 400 MHz spectrometer operating at ambient probe temperature, 283 K, with internal standards for ^{1}H and ^{13}C NMR. External $CFCl_3$ was used to reference ^{19}F NMR spectra. IR spectra were obtained with an Avatar 360 FTIR instrument. Electron impact (EI) and electrospray ionization (ESI) mass spectrometry were performed in the MIT Department of Chemistry Instrumentation Facility.

7′-Chloro-4′-methylfluorescein Dibenzoate (14). 7′-Chloro-4′-methylfluorescein (**13**, 4.8 g, 14 mmol, containing ∼10% 4′,5′-dimethylfluorescein) and benzoic anhydride (13.1 g, 57.9 mmol) were combined in 75 mL of pyridine and refluxed for 2.5 h. The dark brown reaction was cooled to 90 °C and poured into 300 mL of water. The mixture was stirred vigorously, and a brown oily solid formed. The water was replaced periodically, and the oily solid became a light tan powder over the course of ∼2 days. The mixture was filtered, and the powder was dried and taken up in a minimum volume of toluene. The product, which contains ∼10% of 4′,5′-dimethylfluorescein dibenzoate, precipitates as an off-white powder upon addition of EtOH (3.8 g, 41%). TLC $R_f = 0.47$ (silica, CH_2Cl_2). ^{1}H NMR (CD_2Cl_2, 300 MHz) δ 2.37 (2H, s), 6.74 (1H, d, $J = 87$ Hz), 6.94 (1H, d, $J = 8.7$ Hz), 7.00 (1H, s), 7.30 (1H, d, $J = 7.5$ Hz), 7.53−7.59 (4H, m), 7.67−7.80 (4H, m), 8.06 (1H, d, $J = 7.5$ Hz), 8.20−8.24 (4H, m). ^{13}C NMR ($CDCl_3$/DMF-d_7, 125 MHz) δ 7.70, 79.73, 111.89, 111.98, 114.89, 117.01, 117.11, 117.86, 120.68, 122.74, 123.67, 123.76, 124,09, 124.55, 126.78, 127.16, 127.28, 127.33, 127.33, 127.43, 127.49, 128.49, 128.62, 128.74, 129.16, 132.66, 132.94, 134.40, 147.13, 148.14, 149.43, 150.61, 162.09, 162.66, 166.88. FTIR (KBr, cm^{-1}) 1771, 1747, 1600, 1580, 1482, 1466, 1451, 1439, 1409, 1265, 1242, 1217, 1180, 1157, 1081, 1062, 1022, 710, 693. HRMS (ESI) calcd MH$^+$, 589.1054 (major), 590.1088, 591.1025, 592.1059; found, 589.1040 (major), 590.1066, 591.0991, 592.0976.

7′-Chloro-4′-bromomethylfluorescein Dibenzoate (15). A portion (3.7 g, 5.5 mmol) of **14**, 1,1′-azobis(cyclohexanecarbonitrile) (VAZO 88, 172 mg, 0.070 mmol), and 1,3-dibromo-5,5-dimethylhydantoin (1.6 g, 5.5 mmol) were combined in 250 mL of chlorobenzene and stirred. Glacial acetic acid (100 μL) was added, and the reaction was heated to 60 °C for 48 h. The orange solution was extracted with 3 × 250 mL portions of warm water and dried over $MgSO_4$, and the solvent was removed to give an orange solid. The crude material was dissolved in a minimal volume of toluene, and the product, which contains approximately 10% of the bis-(bromomethyl) derivative, precipitates as a peach-colored powder upon addition of EtOH (3.9 g, 95%). TLC $R_f = 0.53$ (silica, CH_2Cl_2). ^{1}H NMR (CD_3OD, 300 MHz) δ 4.80 (2H, s), 6.90 (1H, d, $J = 8.7$ Hz), 7.02 (1H, s), 7.08 (1H, d, $J = 8.7$ Hz), 7.33 (1H, d, $J = 7.5$ Hz), 7.51 (1H, s), 7.54−7.61 (4H, m), 7.69−7.80 (4H, m), 8.07 (1H, d, $J = 7.2$ Hz), 8.22−8.27 (4H, m). ^{13}C NMR (DMF-d_7, 125 MHz) δ 21.43, 80.98, 114.07, 117.40, 119.08, 119.56, 120.15, 122.90, 124.65, 125.63, 125.65, 126.40, 128.53, 128.56, 129.08, 129.26, 129.27, 129.32, 129.43, 129.52, 130.35, 130.47, 130.51, 131.16, 134.72, 134.94, 136.38, 149.15, 149.35, 150.35, 151.36, 152.90, 164.07, 164.20, 168.66. FTIR (KBr, cm^{-1}) 1771, 1746, 1600, 1580, 1482, 1466, 1451, 1439, 1409, 1265, 1242, 1217, 1180, 1157, 1081, 1062, 1022, 899, 796, 710, 693. HRMS (ESI) calcd MNa$^+$, 688.9970, 690.0013 (major), 691.9983, 692.9929; found, 688.9953, 690.9935 (major), 691.9970, 692.9941.

7′-Chloro-4′-fluoresceincarboxaldehyde (16). A portion (4.0 g, 5.3 mmol) of **15** and $NaHCO_3$ (4.5 g, 53 mmol) were combined in 75 mL of DMSO and heated to 150 °C. Over the course of 1 h, the reaction turned from light orange to deep red. After 3 h, the solution was cooled to ∼70 °C and poured into 400 mL of 4 M HCl. A bright orange precipitate formed immediately. After stirring for 2 h, the mixture was filtered, washed with water, and dried. Column chromatography on silica gel (33:1 $CHCl_3$/MeOH) yielded the desired product as a light orange solid, which can be recrystallized from boiling chlorobenzene (463 mg, 22%). TLC $R_f = 0.57$ (silica, 9:1 $CHCl_3$/MeOH); mp = 244−248 °C. ^{1}H NMR (CD_2Cl_2, 300 MHz) δ 6.06 (1H, s), 6.65 (1H, d, $J = 8.7$ Hz), 6.81 (1H, s), 6.90 (1H, d, $J = 8.7$ Hz), 7.05 (1H, s), 7.19 (1H, d, $J = 7.2$ Hz), 7.67−7.70 (2H, m), 8.03 (1H, d, $J = 6.9$ Hz), 10.65 (1H, s), 12.16 (1H, s). ^{13}C NMR (DMF-d_7, 125 MHz) δ 81.67, 104.23, 109.12, 109.90, 111.30, 113.80, 117.75, 124.23, 125.11, 126.57, 128.58, 130.69, 136.00, 136.98, 150.04, 152.35, 153.05, 155.70, 163.99, 168.99, 193.88. FTIR (KBr, cm^{-1}) 1771, 1726, 1653, 1588, 1512, 1467, 1429, 1401, 1359, 1311, 1294, 1263, 1249, 1226, 1151, 1097, 1036, 1000, 892, 878, 841, 794, 772, 762, 727, 703, 646, 625, 543, 532, 486. HRMS (ESI) calcd MH$^+$, 395.0323 (major), 396.0356, 397.0293, 398.0327; found, 395.0308 (major), 396.0354, 397.0286, 398.0325.

2-Nitro-5-fluorobenzylbromide (4). 2-Nitro-5-fluorotoluene (9.3 g, 60 mmol), 1,3-dibromo-5,5-dimethylhydantoin (20 g, 70 mmol), and VAZO 88 (600 mg, 2.5 mmol) were combined in chlorobenzene (600 mL) with stirring. Glacial acetic acid (300 μL) was added, and the solution was stirred at 40 °C for 96 h. The reaction was washed with 3 × 200 mL portions of warm saturated $NaHCO_3$, dried over $MgSO_4$, and filtered, and the solvent was removed under reduced pressure. The crude product is a red-orange solid and consists of approximately 1:1 starting material and product. This material was carried forward to the next step without further purification. Pure **4** can be obtained by column chromatography on silica (6:1 hexanes/EtOAc) as a brown solid (3.84 g, 37%). TLC $R_f = 0.7$ (silica, 4:1 hexanes/EtOAc); mp = 33−34 °C. ^{1}H NMR ($CDCl_3$, 300 MHz) δ 4.83 (2H, s), 7.17 (1H, t, $J = 4.5$ Hz), 7.31 (1H, d, $J = 8.7$ Hz), 8.16 (1H, m). ^{13}C NMR ($CDCl_3$, 125 MHz) δ 33.65, 74.27, 116.60, 119.34, 128.33, 136.17, 166.18. ^{19}F NMR (300 MHz) δ 69.91. FTIR (KBr, cm^{-1}) 3081, 2952, 2865, 1617, 1590, 1529, 1484, 1442, 1414, 1345, 1276, 1251, 1224, 1161, 1139, 1074, 969, 946, 906, 873, 837, 761, 732, 691, 610, 569. HRMS (EI) calcd MH$^+$, 232.9482; found, 232.9497.

1-Fluoro-4-nitro-3-[bis(2-pyridylmethyl)aminomethyl]-benzene (7). A portion (∼7 g, ∼30 mmol, obtained from a 13.9 g mixture containing ∼50% 2-nitro-5-fluorotoluene) of **4**, di(2-picolyl)amine (DPA, 7.4 g, 36 mmol), K_2CO_3 (49 g, 355 mmol), and activated 3 Å molecular sieves were combined in 250 mL of CH_3CN and stirred for 12 h at room temperature. The reaction was filtered through Celite, and the solvent was removed in vacuo to yield a brown oil. Column chromatography on basic Al_2O_3 with a solvent gradient (CH_2Cl_2/EtOAc 9:1 to 4:1 to 7:3) yields the product

as a brown solid (4.8 g, 40%). TLC R_f = 0.63 (Al_2O_3, 3:1 CH_2Cl_2/EtOAc); mp = 72−74 °C. ^{1}H NMR ($CDCl_3$, 300 MHz) δ 3.81 (4H, s), 4.08 (2H, s), 6.99 (1H, m), 7.13 (2H, t, J = 6 Hz), 7.38 (2H, d), 7.63 (3H, m), 7.86 (1H, m), 8.61 (2H, d, J = 6 Hz). ^{13}C NMR ($CDCl_3$, 125 MHz) δ 55.66, 60.25, 114.75, 118.20, 122.61, 123.53, 127.36, 137.17, 138.95, 148.81, 158.13, 163.05, 166.44. ^{19}F NMR (300 MHz) δ 71.88. FTIR (KBr, cm^{-1}) 3109, 3056, 2934, 2852, 1620, 1589, 1519, 1474, 1434, 1364, 1337, 1304, 1262, 1209, 1146, 1065, 958, 904, 845, 824, 773, 761, 684, 620, 581. HRMS (ESI) calcd MH$^+$, 353.1308; found, 353.1414.

4-Amino-1-fluoro-3[bis(2-pyridylmethyl)aminomethyl]-benzene (10). A flask containing Pd/C (10% activated, 2 g) was purged with Ar, and 100 mL of MeOH was added. A portion (1 g, 3 mmol) of **7** was dissolved in 100 mL of MeOH and added to the reaction flask with a syringe. The reaction was stirred vigorously under H_2 (1 atm) for 2 h, purged with Ar, and filtered through Celite, and the solvent was removed in vacuo. Column chromatography on basic Al_2O_3 using a solvent gradient (4:1 CH_2Cl_2/EtOAc to 7:2:1 CH_2Cl_2/EtOAc/MeOH) affords the product as a yellow oil (340 mg, 37%). TLC R_f = 0.58 (Al_2O_3, 3:1 CH_2Cl_2/EtOAc). ^{1}H NMR ($CDCl_3$, 300 MHz) δ 3.63 (2H, s), 3.80 (4H, s), 6.54 (1H, m), 6.79 (2H, m), 7.15 (2H, m), 7.36 (2H, d, J = 7.8 Hz), 7.61 (2H, t, J = 7.8 Hz), 8.55 (2H, d, J = 6 Hz). ^{13}C NMR ($CDCl_3$, 125 Hz) δ 50.50, 57.21, 58.64, 122.94, 113.23, 116.75, 122.87, 123.70, 125.55, 137.74, 148.92, 149.51, 157.37. ^{19}F NMR (300 MHz) δ 44.84. FTIR (NaCl disk, cm^{-1}) 3320, 3214, 2054, 3010, 2923, 2824, 1617, 1590, 1434, 1368, 1287, 1346, 1148, 1093, 1034, 864, 814, 762, 619, 511. HRMS (ESI) calcd MNa$^+$, 345.1486; found, 345.1497.

2-[5-({2-[(Bis(pyridin-2-ylmethyl)amino)methyl]-4-fluorophenylimino}methyl)-2-chloro-6-hydroxy-3-oxo-9,9a-dihydro-3*H*-xanthen-9-yl]-benzoic Acid (Zinpyr-5 Imine, 17). A portion (100 mg, 312 mmol) of **16** was combined with **10** (125 mg, 317 mmol) in 6 mL of EtOAc to yield a pink solution, which was stirred at room temperature for 20 h. A light pink precipitate formed. The mixture was cooled on ice and filtered, and the precipitate was washed with cold EtOAc. The product was used without further purification (135 mg, 62%). ^{1}H NMR (CD_3OD, 400 MHz) δ 3.88 (4H, s), 3.96 (2H, d, J = 6.4 Hz), 6.66 (1H, s), 6.69 (1H, d, J = 6.4 Hz), 6.80 (1H, d, J = 9.0 Hz), 6.99 (1H, s), 7.15 (1H, t), 7.20 (2H, t, J = 2.8 Hz), 7.34 (4H, m), 7.56 (2H, d, J = 7.9 Hz), 7.68 (2H, td, J = 1.7 Hz, J = 7.6 Hz), 7.77 (1H, t, J = 7.77 Hz), 7.83 (1H, t, J = 7.6 Hz), 7.91 (1H, s), 8.08 (1H, d, J = 7.6 Hz), 8.36 (2H, d, J = 4.9 Hz), 9.25 (1H, s). ^{19}F NMR (300 MHz) δ 56.30. FTIR (KBr, cm^{-1}) 3420, 2920, 2849, 1763, 1634, 1594, 1481, 1359, 1271, 1224, 1178, 1151, 1106, 1037, 998, 871, 800, 761, 732, 613, 546, 487. HRMS (ESI) calcd MH$^+$, 699.1811 (major), 700.1844, 701.1781, 702.1815; found, 699.1807 (major), 700.1888, 701.1851, 702.1911.

2-[5-({2-[(Bis(pyridin-2-ylmethyl)amino)-methyl]-4-fluorophenylamino}-methyl)-2-chloro-6-hydroxy-3-oxo-9,9a-dihydro-3*H*-xanthen-9-yl]-benzoic Acid (Zinpyr-5, ZP5, 20). A portion (85 mg, 123 mmol) of **17** was dissolved in 10 mL of DCE, and $NaBH(OAc)_3$ (39 mg, 184 mmol) was added. The reaction was stirred for 2.5 h and changed from cloudy yellow-orange to clear red-orange. The reaction was quenched with 10 mL of saturated brine, and the brine was extracted (3 × 10 mL) with chloroform. The combined organic layers were dried over $MgSO_4$, and the solvent was removed in vacuo to yield a pink solid. A ^{1}H NMR spectrum of the crude material showed >90% purity. Reverse phase column chromatography (65:35 MeOH/0.1 N HCl) followed by solvent removal generated the HCl salt of ZP5, **20**. To obtain the free dye, the HCl salt was loaded onto a second reverse phase column (100% H_2O) and thoroughly washed with H_2O. The product was flushed off the column (100% MeOH), and a portion of the solvent was removed. The remaining solution was taken up in H_2O, washed with hexanes, and dried to yield ZP5 as a red-pink solid (26 mg, 30%). TLC R_f = 0.71 (RP18 silica, MeOH); mp = 99−103 °C. ^{1}H NMR (DMF-d_7, 300 MHz) δ 3.80 (6H, m), 4.60 (2H, s), 6.86 (2H, s), 6.93 (1H, d, J = 8.4 Hz), 6.96 (3H, m), 7.17 (3H, m), 7.45 (3H, t, J = 7.8 Hz), 7.54 (2H, t, J = 7.8 Hz), 7.83 (1H, t, J = 7.2 Hz), 7.89 (1H, t, J = 7.5 Hz), 8.02 (1H, s), 8.09 (1H, d, J = 7.5 Hz), 8.38 (2H, d, J = 3.9 Hz). ^{19}F NMR (300 MHz) δ 45.43. FTIR (KBr, cm^{-1}) 3422, 1664, 1574, 1508, 1460, 1375, 1342, 1307, 1222, 1153, 1009, 939, 886, 835, 765, 716, 630, 598, 549, 468. HRMS (ESI) calcd MH$^+$, 701.1967 (major), 702.2001, 703.1938, 704.1971; found, 701.1963, 702.2001, 703.1967, 704.1952.

2-Nitro-5-chloro-benzylbromide (5). 2-Nitro-5-chlorotoluene (6.0 g, 35.0 mmol), 1,3-dibromo-5,5-dimethylhydantoin (10.6 g, 37.1 mmol), and VAZO 88 (400 mg, 16 mmol) were combined in 275 mL of chlorobenzene and stirred. Glacial acetic acid (200 μL) was added, and the reaction was heated to 40 °C for 120 h. The reaction was extracted (5 × 150 mL) with warm saturated $NaHCO_3$ and washed once with water (150 mL). The organic layer was dried over $MgSO_4$, and the solvent was removed in vacuo to yield a pink-red oily solid that consists of 2-nitro-5-chlorotoluene (~40%) and the desired product (~60%), which was carried on to the next reaction without further purification. Column chromatography on silica gel (25:1 hexanes/EtOAc) yields pure **5** as a brown solid (38%). TLC R_f = 0.51 (silica, 7:1 hexanes/EtOAc); mp = 60−61 °C. ^{1}H NMR ($CDCl_3$, 300 MHz) δ 4.79 (2H, s), 7.45 (1H, dd, J = 3.5, 15.0 Hz), 7.56 (1H, d, 4.0 Hz), 8.0 (1H, d, J = 14.5 Hz). ^{13}C NMR ($CDCl_3$, 300 MHz) δ 28.43, 127.02, 129.61, 132.37, 134.64, 139.91, 145.96. FTIR (KBr, cm^{-1}) 1604, 1569, 1522, 1474, 1443, 1338, 1306, 1227, 1202, 1109, 1064, 908, 827, 757, 706.93, 827, 757, 707, 685, 524. HRMS (EI) calcd M$^+$, 248.9192, 250.9172 (major); found, 248.9186, 250.9152 (major).

2-Nitro-5-chloro-1-[bis(2-pyridylmethyl)aminomethyl]-benzene (8). A portion (~3.5 g, ~14.0 mmol, obtained from a 9.3 g mixture containing ~40% 2-ntiro-5-chlorotoluene) of **5**, DPA (3.32 g, 16.0 mmol), K_2CO_3 (2.6 g, 19 mmol), and 3 Å molecular sieves (3.5 g) were combined in 100 mL of CH_3CN and stirred at room temperature for 24 h. The brown reaction was filtered through Celite, and the solvent was removed in vacuo to yield an impure brown oil. Column chromatography on basic Al_2O_3 using gradient elution (CH_2Cl_2/EtOAc 9:1 to 4:1 to 1:1) yields the product as a brown solid (3.2 g, ~64% based on the assumed composition of the starting mixture). TLC R_f = 0.60 (Al_2O_3, 2:1 CH_2Cl_2/EtOAc); mp = 60−63 °C. ^{1}H NMR ($CDCl_3$, 300 MHz) δ 3.65 (4H, s), 3.92 (2H, s), 6.94 (2H, m), 7.07 (1H, dd, J = 3.0, 14.5 Hz), 7.20 (2H, d, J = 12.3 Hz), 7.44 (2H, td, J = 2.5 Hz, 13.0 Hz), 7.56 (2H, m), 8.28 (2H, d, J = 7.5 Hz). ^{13}C NMR ($CDCl_3$, 125 MHz) δ 55.22, 60.27, 121.89, 122.91, 125.48, 127.47, 130.76, 136.06, 136.67, 138.37, 147.49, 148.59, 157.83. FTIR (KBr, cm^{-1}) 1604, 1589, 1565, 1515, 1474, 1448, 1429, 1363, 1333, 1299, 773, 761, 747. HRMS (ESI) calcd MH$^+$, 369.1118 (major), 370.1152, 371.1089, 372.1123; found, 369.1115, 370.1142, 371.1076, 372.1114.

2-Amino-5-chloro-1-[bis(2-pyridylmethyl)aminomethyl]-benzene (11). To a flask purged with Ar were added Pd/C (10% activated, 1.01 g), 40 mL of MeOH, and a portion (569 mg, 1.55 mmol) of **8** dissolved in 10 mL of MeOH. The reaction was vigorously stirred under H_2 (1 atm) for 1 h at room temperature, purged with Ar, filtered through Celite, and dried in vacuo to yield a brown oil that was used without further purification (380 mg, 72%). The product can be purified by column chromatography on basic Al_2O_3 (20:4:2.5 CH_2Cl_2/EtOAc/^{i}PrNH$_2$) to give a brown oil

(65%). TLC R_f = 0.47 (Al_2O_3, 100:1 CH_2Cl_2/MeOH). ^{1}H NMR ($CDCl_3$, 300 MHz) δ 3.59 (2H, s), 3.80 (4H, s), 6.52 (1H, d, J = 13.5 Hz), 7.00 (2H, m), 7.11 (2H, m), 7.38 (2H, m), 7.60 (2H, td, J = 2.5, 12.5 Hz), 8.55 (2H, d, J = 6.0 Hz). ^{13}C NMR ($CDCl_3$, 125 MHz) δ 57.18, 58.71, 116.62, 121.28, 121.98, 123.20, 123.67, 127.91, 130.29, 136.39, 144.94, 148.64, 158.22. FTIR (NaCl disk, cm^{-1}) 3323, 3211, 3051, 2926, 2820, 1591, 1570, 1493, 1434, 1369, 1298, 1265, 1205, 1150, 1121, 1093, 1049, 997, 975, 895, 868, 820, 758, 731, 701, 643, 552, 487. HRMS (ESI) calcd MH$^+$, 339.1377 (major), 340.1410, 341.1347, 342.1381; found, 339.1383 (major), 340.1417, 341.1335, 342.1364.

2-[5-({2-[(Bis(pyridin-2-ylmethyl)amino)-methyl]-4-chlorophenylamino}-methyl)-2-chloro-6-hydroxy-3-oxo-9,9a-dihydro-3*H*-xanthen-9-yl]-benzoic Acid (Zinpyr-6 Imine, 18). A portion (66 mg, 195 mmol) of **11** was combined with **16** (77 mg, 195 mmol) in 7 mL of EtOAc and stirred at room temperature to yield a cloudy orange-pink solution. A yellow precipitate formed over the course of 12 h. The reaction was cooled on ice and filtered, the precipitate was washed with cold EtOAc, dissolved in 1:1 CH_2Cl_2/MeOH, and washed off the frit, and the solvent was evaporated to afford a pink solid that was used without further purification (67 mg, 48%). ^{1}H NMR (DMF-d_7, 400 MHz) δ 3.10 (4H, s), 3.98 (2H, s), 6.80 (1H, m), 6.92 (3H, m), 7.24 (2H, m), 7.29 (1H, s), 7.50 (5H, m), 7.74 (2H, td, J = 3.0, 12.7 Hz), 7.86 (2H, m), 8.10 (1H, d, J = 12.0 Hz), 8.50 (2H, dq, J = 1.5, 8.5 Hz), 9.48 (1H, s). FTIR (KBr, cm^{-1}) 3432, 3055, 2920, 2849, 1764, 1632, 1613, 1590, 1478, 1433, 1359, 1264, 1225, 1177, 1150, 1090, 1105, 1036, 1013, 871, 799, 762. HRMS (ESI) calcd MH$^+$, 715.1515 (major), 716.1549, 717.1486, 718.1520; found, 715.1532, 716.1567, 717.1522, 718.1557.

2-[5-({2-[(Bis(pyridin-2-ylmethyl)amino)-methyl]-4-chlorophenylamino}-methyl)-2-chloro-6-hydroxy-3-oxo-9,9a-dihydro-3*H*-xanthen-9-yl]-benzoic Acid (Zinpyr-6, ZP6, 21). A portion (67 mg, 95 mmol) of **18** was dissolved in 10 mL of DCE and stirred. $NaBH(OAc)_3$ (25 mg, 118 mmol) was added, and the reaction was left to stir at room temperature. The cloudy orange solution became clear over the course of 5 h. The reaction was washed with 10 mL of saturated brine, and the brine was extracted (3 × 10 mL) with chloroform. The combined organic layers were dried over $MgSO_4$, and the solvent was removed to give **21** as an orange solid (61 mg, 90%). The crude material is ~90% pure. An analytically pure sample was obtained by dissolving ~7 mg of the crude product in 300 μL DMF and adding 1:1 MeOH/0.1% aq TFA (3 mL), which resulted in the immediate precipitation of **21** as an orange solid. TLC R_f = 0.72 (RP18 silica, MeOH); mp = 124−128 °C. ^{1}H NMR (DMF-d_7, 300 MHz) δ 3.75 (6H, m), 4.61 (2H, s), 6.72 (1H, d, J = 15.0 Hz), 6.85 (1H, s), 6.92 (1H, d, J = 15.0 Hz), 7.04 (1H, d, J = 15.5 Hz), 7.20 (4H, m), 7.43 (2H, t, J = 14.0 Hz), 7.56 (2H, t, 12.5 Hz), 7.81−7.94 (2H, dt, J = 13.0, 43.0 Hz), 8.10 (1H, d, J = 13.0 Hz), 8.38 (2H, d, 7.0 Hz). ^{13}C NMR (DMF-d_7, 500 MHz) δ 57.29, 60.23, 83.47, 104.67, 110.45, 111.60, 111.71, 112.95, 113.10, 116.85, 119.46, 122.41, 122.56, 123.45, 124.35, 124.60, 125.17, 127.23, 128.04, 128.47, 128.61, 130.69, 136.00, 136.88, 147.72, 149.22, 149.40, 151.17, 151.45, 152.67, 156.06, 158.97, 159.16, 169.04. FTIR (KBr, cm^{-1}) 3423, 3059, 2805, 1761, 1682, 1471, 1429, 1284, 1255, 1205, 1133, 1072, 1025, 836, 800, 762, 723, 702. HRMS (ESI) calcd MH$^-$, 715.1515 (major), 716.1549, 717.1486, 718.1520; found, 715.1526 (major), 716.1526, 717.1503, 718.1541.

4-Nitro-3-bromomethylanisole (6). 3-Methyl-4-nitroanisole (2.50 g, 15.0 mmol) and 1,3-dibromo-5,5-dimethylhydantoin (5.00 g, 17.5 mmol) were combined in 250 mL of chlorobenzene and stirred. Acetic acid (75 μL, 1.31 mmol) and VAZO 88 (150 mg, 0.614 mmol) were added, and the solution was stirred at 40 °C for 72 h. The crude reaction mixture was washed with 3 × 75 mL portions of warm saturated $NaHCO_3$ (80 °C) and with 75 mL of water. The organic portion was dried over $MgSO_4$ and filtered, and the solvent was removed to give an orange solid. The orange solid, which consists of a mixture of 4-nitro-3-methylanisole (~70%) and the desired product (~30%) was carried on to the next reaction without further purification. Column chromatography on silica gel (15:3:2 hexanes/EtOAc/$C_6H_5CH_3$/EtOAc) yields the pure brominated product as a brown oil (117 mg, 3%). TLC R_f = 0.34 (silica, 4:1 hexanes/EtOAc). ^{1}H NMR ($CDCl_3$, 500 MHz) δ 3.91 (3H, s), 4.82 (2H, s), 6.91 (1H, dd, J = 4.5, 15.0 Hz), 7.02 (1H, d, J = 5.0 Hz), 8.13 (1H, d, J = 15.0 Hz). ^{13}C NMR ($CDCl_3$, 125 MHz) δ 30.19, 56.25, 114.11, 117.69, 127.61, 128.48, 135.72, 163.45. FTIR (NaCl disk, cm^{-1}) 2942, 2845, 1726, 1606, 1582, 1515, 1463, 1438, 1420, 1339, 1295, 1263, 1085, 1030, 836, 758. HRMS (ESI) calcd MH$^+$, 245.9766 (major), 247.9745, 248.9799; found, 245.9760 (major), 247.9743, 248.9773.

4-Nitro-3-[bis(2-pyridylmethyl)aminomethyl]-anisole (9). A portion (~1.1 g, ~4.6 mmol, obtained from a 3.56 g mixture containing ~70% 3-methyl-4-nitroanisole) of **6**, DPA (950 mg, 4.77 mmol), K_2CO_3 (6.50 g, 47.0 mmol), and powdered molecular sieves (750 mg) were combined in 20 mL of CH_3CN and stirred for 12 h at room temperature. The reaction was filtered through Celite, and the solvent was removed in vacuo to yield a brown oil. Column chromatography on basic Al_2O_3 with a solvent gradient (CH_2Cl_2/EtOAc 9:1 to 4:1 to 7:3) affords the product as an orange oil (954 mg, 57%). TLC R_f = 0.32 (Al_2O_3, 3:1 CH_2Cl_2/EtOAc). ^{1}H NMR ($CDCl_3$, 500 MHz) δ 3.84 (4H, s), 3.88 (3H, s), 4.14 (2H, s), 6.77 (1H, dd, J = 2.5, 8.5 hz), 7.13 (2H, td, J = 1.5, 5.0 Hz), 7.43 (2H, d, J = 7.5 Hz), 7.50 (1H, d, J = 3.0 Hz), 7.62 (2H, td, J = 1.0, 5.0 Hz), 7.92 (1H, d), 8.51 (2H, dq). ^{13}C NMR ($CDCl_3$, 125 MHz) δ 56.06, 56.40, 112.84, 115.65, 122.32, 123.18, 127.49, 136.68, 138.46, 142.50, 149.20, 158.90, 163.27. FTIR (NaCl disk, cm^{-1}) 3066, 3010, 2926, 2841, 1589, 1513, 1433, 1340, 1284, 1236, 1080, 842, 763. HRMS (ESI) calcd MH$^+$, 365.1614; found, 365.1608.

3-[Bis(2-pyridylmethyl)aminomethyl]-*p*-anisidine (12). To a flask purged with Ar was added Pd/C (10% activated, 1.0 g), **9** (914 mg, 2.51 mmol), and 200 mL of MeOH. A balloon of H_2 was attached to the reaction which was left to stir for 12 h at room temperature. The reaction was filtered through Celite, and the solvent was removed to yield a dark yellow oil. Column chromatography on basic Al_2O_3 with a solvent gradient (9:1 CH_2Cl_2/EtOAc to 4:1 CH_2Cl_2/EtOAc to 7:2:1 CH_2Cl_2/EtOAc/MeOH) followed by a second column packed with basic Al_2O_3 (99:1 $CHCl_3$/MeOH) affords the product as an orange oil (466 mg, 56%). TLC R_f = 0.82 (4:1 CH_2Cl_2/EtOAC). ^{1}H NMR ($CDCl_3$, 500 MHz) δ 3.63 (2H, s), 3.73 (3H, s), 3.80 (4H, s), 4.56 (2H, bs), 6.57 (1H, d, J = 8.5 Hz), 6.64−6.69 (2H, m), 7.15 (2H, t, J = 5.0 Hz), 7.39 (2H, d, J = 8.0 Hz), 7.62 (2H, td, J = 2.0, 7.5 Hz), 8.55 (2H, dt, J = 1.0, 5.0 Hz). ^{13}C NMR ($CDCl_3$, 125 MHz) δ 55.96, 58.02, 60.38, 113.94, 116.65, 117.26, 122.23, 123.61, 123.99, 136.54, 140.76, 149.32, 151.97, 159.34. FTIR (NaCl disk, cm^{-1}) 3412, 3319, 3217, 2933, 2829, 1590, 1569, 1503, 1433, 1253, 1150, 1046, 764. HRMS (ESI) calcd MH$^+$, 335.1872; found, 335.1794.

9-(*o*-Carboxyphenyl)-2-chloro-5-[2-{bis(2-pyridylmethyl)aminomethyl}-*N*-(*p*-anisidine)]-6-hydroxy-3-xanthanone (Zinpyr-7, ZP7, 23). 2′-Chloro-5′-bromomethyl-fluorescein di-*tert*-butyldimethylsilyl ether (**22**, 340 mg, 494 μmol) and pyridine (304 mg, 1.48 mmol) were combined in 20 mL of CH_3CN and stirred. Silver nitrate (92 mg, 541 μmol) was added, causing the reaction to change from yellow to clear with the formation of a white precipitate. After 10 min, 3-[bis(2-pyrdylmethyl)aminomethyl]-*p*-anisidine (199 mg, 595 μmol) dissolved in 10 mL of CH_3CN was added, and the reaction mixture was stirred for 12 h at room temperature. The

crude reaction mixture was filtered through Celite, and the solvents were evaporated to yield TBS-protected ZP7. The crude product was combined in 15 mL of THF with AcOH (30 mL, 5048 μmol) and 1.0 M tetrabutylammonium fluoride (TBAF in THF, 350 μL, 350 μmol), and the solution was stirred. Upon addition of TBAF, the solution immediately changed from orange to deep red. After 24 h, the reaction was diluted with 75 mL of H_2O, and the aqueous portion was washed (2 × 100 mL) with hexanes and then saturated with NaCl. The product was extracted into EtOAc, washed with H_2O (100 mL) and brine (3 × 100 mL), dried over Na_2SO_4, and filtered, and a red solid was obtained after solvent removal. Column chromatography using reverse phase silica gel (3:1 CH_3CN/0.1 N HCl followed by removal of CH_3CN yielded an acidic solution of ZP7. This solution was loaded onto a second RP18 silica column packed with water. The column was thoroughly washed with water, and 4:1 CH_3CN/H_2O was used to wash ZP7 off the column. An orange powder was obtained after solvent removal (69 mg, 20%). TLC R_f = 0.32 (RP18, MeOH); mp = 104−110 °C. ^{1}H NMR (CD_3CN, 500 MHz) δ 3.63 (2H, d, J = 1.5 Hz), 3.66 (3H, s), 4.64 (1H, d, J = 14.5 Hz), 4.68 (1H, d, J = 14.5 Hz), 6.52 (1H, d, J = 8.5 Hz), 6.57 (1H, d, J = 9.0 Hz), 6.67 (1H, dd, J = 3.0, 9.0 Hz), 6.75−6.77 (2H, m), 6.80 (1H, s), 6.97 (1H, s), 7.13 (2H, td, J = 1.0, 4.0 Hz), 7.23 (1H, d, J = 7.5 Hz), 7.27 (2H, d, J = 8.0 Hz) , 7.56 (2H, td, J = 2.0, 7.5 Hz), 7.70 (1H, td, J = 1.0, 7.5 Hz), 7.76 (1H, td, J = 1.0, 7.5 Hz), 7.99 (1H, d, J = 8.0 Hz), 8.42 (2H, d, J = 4.0 Hz). FTIR (KBr, cm^{-1}) 3333, 3061, 2830, 1760, 1636, 1598, 1511, 1451, 1371, 1283, 1252, 1218, 1152, 869, 763. HRMS (ESI) calcd MH^+, 713.2167 (major), 714.2201, 715.2138, 716.2171; found, 713.2188 (major), 714.2201, 715.212, 716.2182.

General Spectroscopic Methods. Ultrol grade PIPES, piperazine-*N*,*N*′-bis(2-ethanesulfonic acid), from Calbiochem, KCl (99.997%), and $ZnCl_2$ (99.999%) were used as received. Millipore water was used for all aqueous solutions, which were filtered through 0.2 mm cellulose filters prior to use. With the exception of the experiment to determine pK_a values, all spectroscopic measurements were conducted under simulated physiological conditions using 50 mM PIPES, 100 mM KCl adjusted to pH 7. An Orion glass electrode, calibrated prior to each use, was used to record solution pH. Zinc solutions were prepared from 100 mM stock solutions in water. Stock solutions of ZP5 (0.76 μM), ZP6 (0.41 μM), and ZP7 (0.67 μM) in DMSO were prepared, stored frozen at −25 °C, and thawed in the dark immediately prior to use. The KaleidaGraph software package was used to manipulate all spectral data.

Optical Absorption Spectroscopy. UV−vis spectra were obtained with a Cary 1E scanning spectrophotometer, and a circulating water bath was used during all acquisitions to maintain the temperature at 25 ± 1 °C. Samples were contained in 1-cm path length quartz cuvettes (3.5 mL volume). All manipulations were performed in triplicate.

Zn(II) Binding Studies (Absorption Spectroscopy). Metal-binding titrations and Job plots were obtained for ZP5, ZP6, and ZP7 to determine the stoichiometry of the metal-bound complexes in solution. In a typical titration, 0.5 μL aliquots of a 10 mM $ZnCl_2$ solution were added to a 3 mL solution of ZP (concentration range 10−20 μM). The absorbance changes at 512 (ZP5, ZP6, ZP7), 491 (ZP5), 492 (ZP5, ZP7), and 462 (ZP5, ZP6, ZP7) nm were recorded and plotted against the equivalents of Zn(II) in solution. For the Job plot analyses, a 10 μM solution of Zn(II) in 50 mM PIPES, 100 mM KCl, pH 7 was prepared from a 10 mM stock solution in water, and a titration (reciprocal dilution) was performed starting with a 10 mM ZP solution (3 mL). A^* was calculated for a minimum of three different wavelengths according to the equation $A^* = A_{observed} - \epsilon_{Zinpyr} \times [ZP]$, where ZP refers to the metal-free probe, and plotted against the mol fraction of Zn(II) in solution.

Fluorescence Spectroscopy. Emission spectra were recorded on a Hitachi F-3010 spectrofluorimeter. A rhodamine quantum counter was used to normalize the spectra for excitation intensity, and manufacturer-supplied correction curves were utilized to normalize the emission spectra. Manufacturer-supplied photomultiplier curves were used to correct for emission intensity. The temperature was regulated at 25 ± 1 °C during all experiments with a circulating water bath. All spectra were obtained by using 3 nm slit widths, and samples were contained in a 1 cm × 1 cm quartz cuvette (3.5 mL volume). Measurements were conducted with three or more repetitions.

Quantum Yield Measurements. The quantum yields of the ZP5, ZP6, and ZP7 were referenced to fluorescein in 0.1 N NaOH (ϕ = 0.95).[58] In a typical experiment, a 6 mL solution of 1 μM Zinpyr was prepared in 50 mM PIPES, 100 mM KCl, pH 7. For metal-free studies, 6 mL of 100 mM K_4EDTA was added to chelate any adventitious metal ions. To determine the quantum efficiencies of the metal-bound dyes, either 2 mL (ZP5) or 6 mL (ZP6, ZP7) of a 100 mM $ZnCl_2$ stock solution was added to a 1 μM ZP solution. Excitation was provided at 497 nm (ZP5 and ZP6, metal-free), 491 nm (ZP5, metal-bound), or 493 nm (ZP6, metal-bound). Emission spectra were integrated from 450 to 650 nm, and the quantum yields were calculated by standard methods.[53]

Determination of Protonation Constants That Affect Fluorescence. The pK_a values that affect fluorescence were determined by plotting the integrated emission intensity versus pH from ∼12.5 to ∼2. In a typical experiment, a 30 mL solution of 1 μM ZP in 100 mM KCl, 10 mM KOH was adjusted to pH 12.5 by dropwise addition of KOH. Aliquots of 6, 2, 1, 0.5, and 0.01 N HCl were added to achieve pH changes of approximately 2.5, and the emission spectrum was gathered after each addition. The overall volume change for each experiment did not exceed ∼2%. Excitation was provided at 498 nm for ZP5 and ZP7 and at 500 nm for ZP6. Data were integrated from 505 to 650 nm, normalized, and plotted against pH. The data were fit to the nonlinear expression previously described.[53]

Selectivity of ZP for Zn(II) in the Presence of Other Metal Ions. The metal ion selectivity of ZP5 and ZP6 for a number of divalent first-row transition metals, in addition to Ca(II), Mg(II), and Cd(II), was investigated by using fluorescence spectroscopy. Aqueous solutions for Ca(II), Mg(II), Mn(II), Co(II), Ni(II), and Cd(II) were prepared from the chloride salts. The Cu(II) solution was prepared from copper sulfate, and Fe(II) solutions were prepared immediately before use with ferrous ammonium sulfate and water that was thoroughly purged with Ar. In a typical experiment, the emission spectrum of a 1 μM solution of free dye was recorded. A 15 μL aliquot of ∼10 mM metal ion solution was added and the emission spectrum recorded. Subsequently, 15 μL of 10 mM $ZnCl_2$ was added to the solution and the emission spectrum obtained. Excitation was provided at 498 nm (ZP5) or 500 nm (ZP6), and the spectra were integrated from 505 to 650 nm (ZP5) or from 450 to 650 nm (ZP6).

Zn(II) Binding Studies by Fluorescence Spectroscopy. The dissociation constants, K_d, for Zn(II) binding were determined with a dual-metal buffering system,[52] which affords concentrations of free Zn(II) in the nanomolar range. Excitation was provided at 498 nm for ZP5 and at 500 nm for ZP6. The response was quantified by integrating the emission intensity from 505 to 650 nm and normalizing. The plot of response versus [Zn] was fit to the equation

(58) Brannon, J. H.; Magde, D. *J. Phys. Chem.* **1978**, *82*, 705−709.

Scheme 1

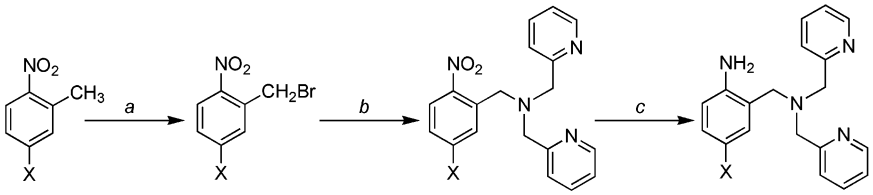

(*a*) 1,3-Dibromo-5,5-dimethylhydantoin, VAZO 88, HOAc, chlorobenzene, 40 °C
(*b*) DPA, K_2CO_3, CH_3CN, rt
(*c*) Pd/C (10% activated), H_2 (1 atm), MeOH, rt

Scheme 2

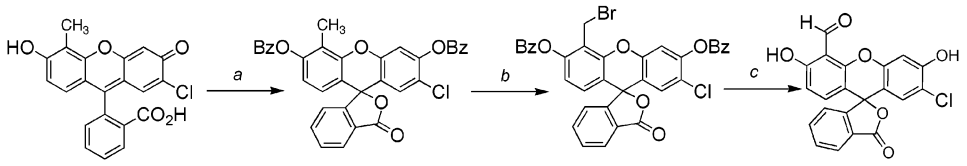

(*a*) Benzoic anhydride, pyridine, 150 °C
(*b*) 1,3-Dibromo-5,5-dimethylhydantoin, VAZO 88, HOAc, chlorobenzene, 40 °C
(*c*) $NaHCO_3$, DMSO, 150 °C

$r = B[\mathrm{Zn}]/(K_d + [\mathrm{Zn}])$, where r is the fluorescence response and B is 1 for normalized data.[52]

HeLa Cell Preparation and Fluorescence Microscopy. HeLa cells were plated on untreated 6-well plates and grown to 60% confluence in DMEM (2 mL) supplemented with 10% fetal bovine serum. Each ZP dye was introduced directly to the medium from the DMSO stock solutions previously described to yield final concentrations of 5 μM ZP. The cells were incubated with the dye for 30 min at room temperature and washed with 2 × 2 mL portions of PBS before imaging. For the addition of Zn(II), HeLa cells treated with ZP were bathed in 2 mL of DMEM, and 10 μL of a 10 mM Zn-pyrithione solution in DMSO was added. The cells were incubated for 10 min at room temperature and washed with 2 × 2 mL portions of PBS before imaging. ZP1 and ZP1 + Zn(II) were used as positive controls. A Nikon Eclipse TS100 fluorescence microscope outfitted with a 100 W mercury lamp was used for imaging.

Results and Discussion

Syntheses of Ligand Components. The syntheses of the ligand-binding units for ZP5−7, starting from commercially available materials, are outlined in Scheme 1. Free radical bromination of the 5-substituted 2-nitrotoluenes under mild conditions achieves multigram quantities of the corresponding brominated derivatives. These bromination reactions are sluggish, progressing over the course of several days until no additional product formation is observed. The final starting material-to-product ratio varies depending on the substituent, ranging from 70% (ZP7) to 40% (ZP6). Although the fluoro and chloro derivatives can be easily separated from their corresponding starting materials by flash chromatography, the methoxy species, **6**, is unstable to column chromatography and is isolated in extremely low yield (3%) after purification. This separation, however, is not required since the starting substituted toluenes do not interfere with the next step. The reaction of **4**−**6** with DPA in CH_3CN followed by purification and hydrogen reduction of the nitro to an amino group using Pd/C (10% activated) as a catalyst yields the aniline-based ligand fragments **10**−**12** with overall yields of ∼5% (ZP5), ∼28% (ZP6), and ∼10% (ZP7).

Monofunctionalized Fluorophore and ZP Syntheses. Previously described syntheses of ZP probes followed one of three main routes. Mannich reactions between a fluorescein with halogen substitution at the 2′ and 7′ positions and the imminium ion condensation product of DPA and paraformaldehyde offer a simple and high yielding approach to symmetrical ZP sensors (ZP1−3).[55] This method, however, is limited to ligands that incorporate a secondary amine. In an alternative synthesis of symmetrical ZP sensors, a disubstituted fluorescein was created in four steps starting from 2-methylresorcinol and phthalic anhydride.[53] The two carboxaldehyde groups in the 4′ and 5′ positions of the fluorescein offer more flexibility for subsequent ligand attachment strategies. In order to achieve unsymmetrical ZP sensors that will form mononuclear Zn(II) complexes in solution, we described a four-step synthesis for 2′-chloro-5′-bromomethylfluorescein di-*tert*-butyldimethylsilyl ether, **22**, which was used as the platform in the assembly of ZP4.[54]

In the present work we have developed a second unsymmetrical fluorescein platform, **16**, that incorporates an aldehyde functional group in the 4′ position, the synthesis of which is depicted in Scheme 2. Reaction of 7′-chloro-4′-methylfluorescein, **13**, (containing ∼10% 4′,5′-dimethylfluorescein) with 4 equiv of benzoic anhydride in refluxing pyridine affords the benzoate protected species, **14**, in moderate yield (41%, with ∼10% 4′,5′-dimethylfuorescein dibenzoate). Free radical bromination under standard conditions yields the corresponding benzylbromide, **15**, in high yield (95%, containing ∼10% of 4′,5′-dibromomethylfluorescein dibenzoate), and multigram quantities of **15** can be readily obtained. Oxidation of **15** in DMSO with an excess of $NaHCO_3$ yields the desired aldehyde function-

Scheme 3

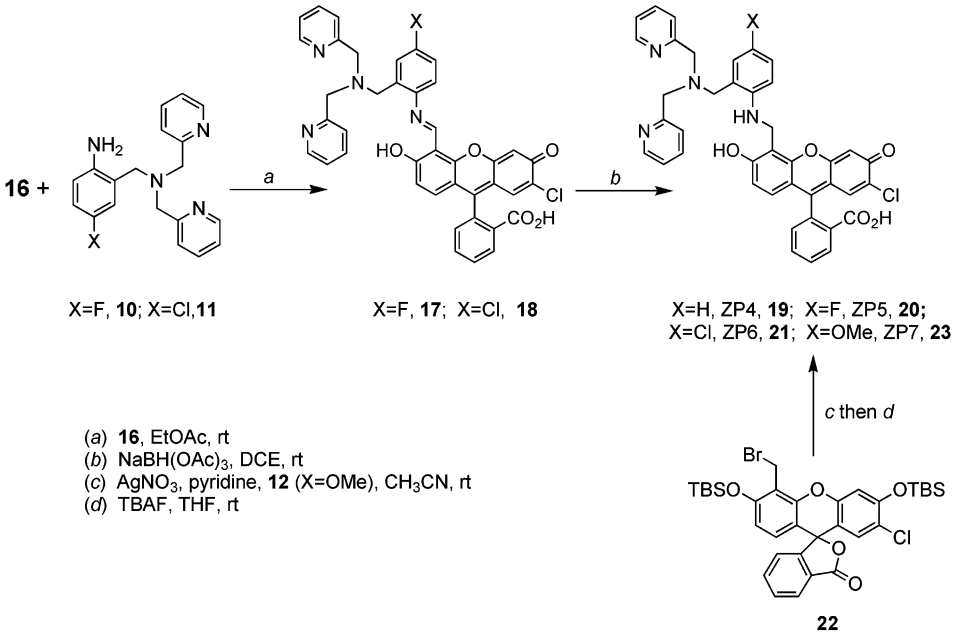

alized fluorescein, **16**, in 21% yield after purification by column chromatography. This platform offers several advantages for the convergent synthesis of fluorescein-based sensors. Since aniline-type nitrogen atoms are relatively unreactive toward nucleophiles, in situ generation of the nitroxyl fluorescein species is required to assemble ZP4 using the 7′-chloro-4′-bromo-methylfluorescein di-*tert*-butyldimethylsilyl ether platform. The carboxaldehyde functionality in **16** facilitates imine condensations and subsequent reductions for coupling aniline-based ligands to a fluorescein platform. Since the benzoate protecting groups are cleaved off during the DMSO oxidation, deprotection is not required after installation of the ligand moiety.

The utility of the 7′-chloro-4′-fluoresceincarboxaldehyde building block was explored in the syntheses of ZP5 and ZP6, which are shown in Scheme 3. In both cases, condensation of **10** or **11** with **16** in dry EtOAc resulted in precipitation of the corresponding Schiff base, **17** or **18**, in high purity. Reduction of each imine with a slight excess of $NaBH(OAc)_3$ in DCE afforded the final sensors, a reaction that can be monitored by the changes in color and solution clarity. The purity of the crude ZP compounds obtained from this route is high (∼90%). Pure ZP6 was obtained by precipitation from DMF upon addition of a methanol/aqueous TFA mixture. Reverse phase column chromatography with 4:1 MeOH/0.1 N HCl followed by a second column packed with 100% water was used to achieve pure ZP5 in 30% yield. In contrast, ZP7 was assembled by reaction in CH_3CN with the nitroxyl derivative of **22**, generated in situ by addition of $AgNO_3$, see Scheme 3.[54] Removal of the silyl protecting groups was accomplished by addition of TBAF in THF. ZP7 was purified analogously to ZP5 by using 3:1 CH_3CN/0.1 N HCl as the eluent for the first column and was obtained in 20% yield.

Fluorescence Properties of ZP5, ZP6, and ZP7. The fluorescence properties of the unsymmetrical ZP sensors are summarized in Table 1. Under simulated physiological conditions (50 mM PIPES, 100 mM KCl, pH 7), and in the presence of EDTA to scavenge any adventitious metal ions, ZP5, ZP6, and ZP7 have quantum efficiencies of 0.29, 0.10, and 0.04, respectively, and exhibit maximum emission at 520, 519, and 521 nm. Upon addition of excess Zn(II), the quantum yields of ZP5 and ZP6 increase, affording values of 0.48 and 0.34, respectively. When the dual-metal buffering system is employed to achieve free Zn(II) concentrations from 0 to 25 nM, ZP5 shows a ∼1.6-fold increase and ZP6 a ∼3-fold increase in integrated emission. The emission maximum of both ZP5 and ZP6 blue-shift slightly to 517 nm (ZP5) and 515 nm (ZP6) upon Zn(II) coordination. Although the emission maximum of ZP7 displays a comparable blue-shift to 517 nm, the fluorescence enhancement of ZP7 upon addition of excess Zn(II) is negligible; the quantum yield of the Zn(II) bound sensor is only 0.05. For each ZP sensor, concomitant blue-shifts of ∼10 nm occur in the optical spectra as a result of Zn(II) complexation. For ZP5, the absorption maximum shifts by 9 nm from 504 nm (ϵ = 82 500 M^{-1} cm^{-1}) to 495 nm (ϵ = 91 000 M^{-1} cm^{-1}) upon introduction of 1 equiv of Zn(II). ZP6 shows a comparable shift, from 506 nm (ϵ = 88 600 M^{-1} cm^{-1}) to 495 nm (ϵ = 98 000 M^{-1} cm^{-1}), and the absorption

Table 1. Properties of Unsymmetric ZP Sensors

	X	ϕ_f[b]	ϕ_{Zn}[c]	ϵ[d] (M^{-1} cm^{-1})	ϵ[e] (M^{-1} cm^{-1})	pK_a[f]	pK_a[g]	pK_a[h]
ZP4[a]	H	0.06	0.34	61 000	66 700	4.0	7.2	10.0
ZP5	F	0.29	0.48	82 000	91 000	4.7	9.6	10.9
ZP6	Cl	0.10	0.34	88 600	98 000	4.7	6.3	11.2
ZP7	OMe	0.04	0.05	68 800	77 400	4.6	6.9	

[a] Taken from ref 53. [b] The quantum yield of the free dye relative to fluorescein in 0.1 N NaOH. [c] The quantum yield of the Zn(II) complex relative to fluorescein in 0.1 N NaOH. [d] Absorbance at 504 nm, ZP5; 506 nm, ZP6; 505, nm ZP7. [e] Absorbance at 495 nm for all ZP sensors. [f] Corresponds to formation of a nonfluorecent isomer of fluorescein, see Figure 2 and Scheme 4. [g] The pK_a of the aniline nitrogen atom responsible for PET quenching in the unbound dye. [h] The pK_a of the tertiary amine.

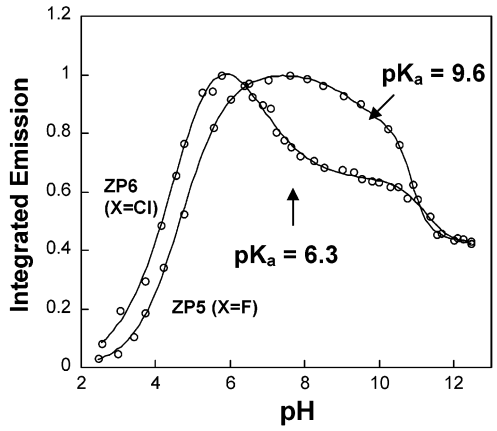

Figure 2. Normalized integrated emission versus pH for ZP5 and ZP6. $\lambda_{ex} = 498$ nm, ZP5; $\lambda_{ex} = 500$ nm, ZP6. Emission data was integrated from 505 to 650 nm and normalized. The pK_a values given in the plot are for the aniline nitrogen atom. See Table 1 for complete data and Figure S1 for the pK_a titration for ZP7.

maximum for ZP7 shifts from 505 nm ($\epsilon = 68\,000$ M^{-1}cm^{-1}) to 495 nm ($\epsilon = 77\,400$ M^{-1} cm^{-1}). These hypsochromic shifts reflect a perturbation of the fluorescein π-system and suggest that the phenol donor group of the fluorescein coordinates to Zn(II), as observed for ZP1, ZP2, and ZP4.[53,54] The brightness ($\phi \times \epsilon$) of ZP5 increases 1.8-fold from 23 900 M^{-1} cm^{-1} to 43 700 M^{-1} cm^{-1} upon Zn(II) coordination. The brightness of ZP6 increases 3.8-fold from 8900 M^{-1} cm^{-1} to 33 000 M^{-1} cm^{-1}, and ZP7 shows a 1.4-fold brightness change, from 2800 M^{-1} cm^{-1} to 3900 M^{-1}cm^{-1}; however, the increase in brightness for ZP7 is primarily due to an increase in the molar absorptivity, not in the quantum yield.

Our previous work on symmetrical ZP sensors and ZP4 revealed a correlation between the quantum yields of apo ZP probes and the pK_a values of the nitrogen atom responsible for PET quenching. Our objective here is to extend this correlation through comparison of quantum yields and aniline nitrogen pK_a values for ZP5−7, asymmetrical ZP4-like sensors with substituents para to the atom responsible for PET. In Figure 2, we illustrate the pH-dependent fluorescence changes for ZP5 and ZP6. The corresponding plot for ZP7 is given in Figure S1 of Supporting Information. The fluorescence of ZP6 is ∼50% quenched at high pH and increases in the physiological range, reaching a maximum around pH 5. ZP6 fluorescence is affected by three protonation events with apparent pK_a values of 11.2, 6.3, and 4.7. The first two values correspond to fluorescence enhancement and are assigned to the tertiary amine and aniline nitrogen, respectively, whereas the latter is associated with fluorescence quenching and the formation of a nonfluorescent isomer. These protonation events are depicted in Scheme 4. Although the electron-withdrawing Cl substituent in ZP6 lowers the aniline nitrogen atom pK_a relative to that in ZP4 (X = H, pK_a = 7.2), the quantum yield of ZP6 is slightly greater than that of ZP4 ($\phi = 0.06$ for ZP4, 0.10 for ZP6). The fluorescence of ZP7, similar to that of ZP4 and ZP6, is effectively quenched at high pH and increases in the physiological range, see Figure S1. From the pH range used in this analysis, we are able to observe only two protonation

Scheme 4

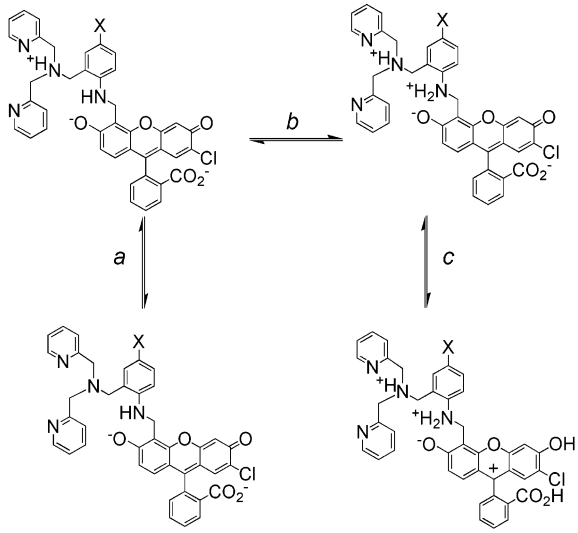

(a) Protonation of the tertiary amine. Not observed for ZP7. (b) Protonation of the aniline nitrogen atom responsible for PET. (c) Formation of a non-fluorescent isomer at low pH.

events. The pK_a of ZP7 at 6.9 corresponds to protonation of the aniline nitrogen atom, and the pK_a at 4.6 results in formation of a nonfluorescent isomer as shown in Scheme 4. In contrast, the emission of ZP5 reaches a maximum around pH 8 and is maintained throughout the physiological range. Three protonation events affect the fluorescence of ZP5 and have apparent pK_a values of 10.9, 9.6, and 4.7. The pK_a of 10.9 is assigned to the aliphatic amine, and the pK_a of 4.7 corresponds to formation of a nonfluorescent isomer. The pK_a of 9.6 is assigned to the aniline nitrogen atom, protonation of which at physiological pH inhibits PET quenching of free ZP5 and causes its relatively high background fluorescence ($\phi = 0.29$). Variation of X clearly has little effect on the pK_a values for the aliphatic amine and for formation of the nonfluorescent isomers. In contrast, the pK_a of the aniline nitrogen atom is sensitive to changes in X, especially when X = F, and these variations generally follow the relative quantum yields of the metal-free probes.

The fluorescence response of ZP5 and ZP6 to various divalent first-row transition metal ions, Zn(II), and Cd(II), is shown in Figure 3. Both compounds exhibit similar behavior. ZP5 and ZP6 fluorescence enhancement is specific for Zn(II) and Cd(II) and unaffected by the presence of excess Ca(II), Mg(II), and Mn(II). ZP5 and ZP6 form complexes with the divalent first-row transition metals Fe(II), Co(II), Ni(II), and Cu(II). Complexation of ZP5 and ZP6 to these metal ions results in no appreciable fluorescence change. When Zn(II) is added to solutions of ZP5 or ZP6 and a divalent first-row transition metal of interest (see Figure 3), the Zn(II)-induced fluorescence enhancement is not observed, indicating that Zn(II) is unable to displace Fe(II), Co(II), Ni(II), or Cu(II) from the ZP probes. Analogous behavior is observed for the sensor ZP4.[54] Since ZP7 shows only a negligible fluorescence change upon addition of Zn(II), the metal ion selectivity experiments were not conducted with ZP7.

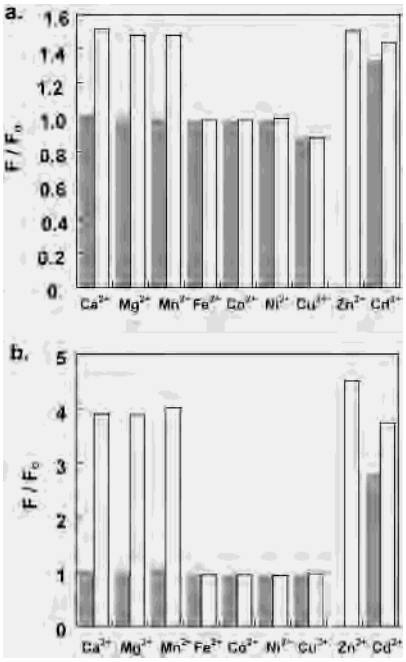

Figure 3. The selectivity of ZP5 and ZP6 for Zn(II) in the presence of other metal ions at pH 7 in 50 mM PIPES, 100 mM KCl. The response is normalized with respect to the background fluorescence of the free dye (F_o). Dark bars: A 1 μM solution of ZP containing 50 equiv of M(II). Colorless bars: Subsequent addition of 50 equiv of Zn(II) to the solution containing ZP and the cation of interest. (a) ZP5, $\lambda_{ex} = 498$ nm, and the emission was integrated from 505 to 650 nm. (b) ZP6, $\lambda_{ex} = 500$ nm, and the emission was integrated from 450 to 650 nm. The fluorescence response of ZP5 and ZP6 is also unaffected by millimolar concentrations of K(I), Ca(II), and Mg(II).

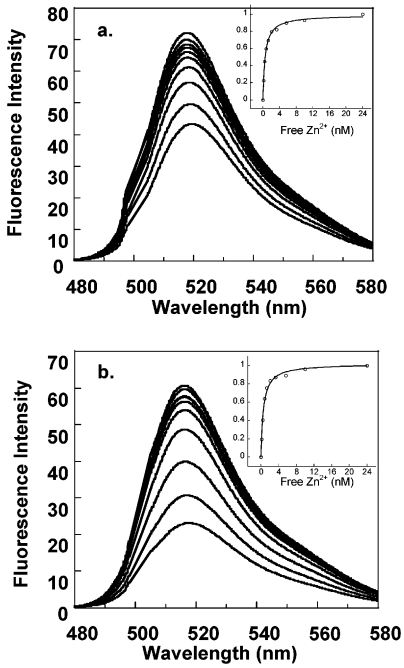

Figure 4. Fluorescence enhancement of ZP probes upon addition of buffered Zn(II) solutions at pH 7 in 50 mM PIPES, 100 mM KCl. The concentration of ZP is 500 nM, and the concentrations of free Zn(II) are 0.0, 0.17, 0.42, 0.79, 1.3, 2.1, 3.4, 5.6, 10.2, and 24 nM. (a) ZP5, $\lambda_{ex} = 498$ nm. (b) ZP6, $\lambda_{ex} = 500$ nm. Insets: Emission response (*y*-axis) obtained by integrating the emission spectra, subtracting the spectrum of the free dye of interest, and normalizing to the full response.

Zn(II)-Binding Properties of ZP5, ZP6, and ZP7. The binding affinities of ZP5 and ZP6 for Zn(II) were determined by using the dual-metal buffering system previously described.[52] In this system, the concentrations of Ca(II) and EDTA remain constant at 2 and 1 mM, respectively, while the total Zn(II) concentration varies from 0 to 1 mM, which affords solutions that contain 0−25 nM of free Zn(II). Figure 4 shows the emission response from titrations of ZP5 and ZP6 with the dual-metal buffering system. ZP5 exhibits a ~1.6-fold increase in integrated emission, and the Zn(II) complex has an apparent K_d of 0.50 ± 0.10 nM. The integrated emission intensity for ZP6 increases ~3-fold, and analysis of the response shows that the Zn(II) complex also has an apparent K_d of 0.50 ± 0.10 nM. Formation of the 1:1 Zn(II)/ZP complex is responsible for the Zn(II)-induced fluorescence enhancement for both ZP5 and ZP6.

Titrations of ZP5 and ZP6 with Zn(II) and Job plot analyses were performed to characterize Zn(II) complexation. These data are given in Figure S2 of Supporting Information. The difference spectra obtained from titration of ZP5 or ZP6 with 10 mM Zn(II) show comparable features. An absorption decrease at 512 nm and increases at 492 and 462 nm occur upon addition of Zn(II). Titrations of ZP5 and ZP6 with Zn(II) indicate 1:1 stoichiometry in solution, and the Job plots show breaks at 0.5, also indicative of 1:1 binding. Job analyses of ZP5 with Mn(II) and Cu(II) were also performed and give analogous results, as presented in Figure S3 of Supporting Information. Since the fluorescence enhancement of ZP7 is negligible, a comparison of its optical spectrum

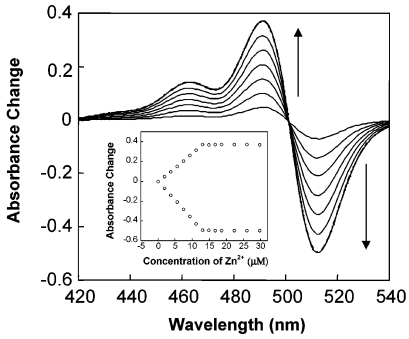

Figure 5. UV−vis difference spectra resulting from the addition of Zn(II) to ZP7 in 50 mM PIPES, 100 mM KCl, pH 7. The concentration of ZP7 is 13 μM. Increases in absorption at 462 and 492 nm and a decrease in absorption at 512 nm occur as a result of Zn(II) binding. Inset: Change in absorbance versus concentration of Zn(II) at 512 and 492 nm. The break at 13 μM Zn(II) indicates formation of a 1:1 complex with ZP7.

with those of ZP5 and ZP6 is worthwhile to illustrate similarities in Zn(II) binding. The difference spectrum for a metal binding titration of ZP7 with Zn(II) is depicted in Figure 5, and those for ZP5 and ZP6 are shown in Figure S3 of Supporting Information. Like ZP5 and ZP6, addition of Zn(II) to a solution of ZP7 indicates that the dye binds the metal ion with a 1:1 stoichiometry and with analogous changes in optical spectra. These observations demonstrate that ZP7 binds Zn(II) in an identical manner and with similar affinity.

Comparison of ZP5, ZP6, and ZP7 to Other ZP Sensors. ZP5, ZP6, and ZP7 are the most recent additions to the ZP family of Zn(II) sensors and are based on the unsymmetrical ZP4 motif. These intensity-based sensors contain one Zn(II) binding site, which incorporates four

nitrogen donors and the phenolate oxygen of the fluorescein platform. They operate via a photoinduced electron transfer (PET) mechanism.[56,57] The lone pair on the secondary nitrogen atom donates an electron into the excited state of the fluorophore, which quenches the fluorescein fluorescence in the metal-free form. Upon coordination to Zn(II), the lone pair electron is no longer available to quench the fluorophore excited state, and emission occurs. Investigation of these dyes, and others,[59] illustrates the relationship between the pK_a of the donor nitrogen atom and the extent of PET quenching in the unbound sensor. ZP1 and ZP2, symmetrical fluorescein-based sensors that incorporate two DPA binding units linked to the fluorophore through a benzylic amine, display considerable background fluorescence in the unbound form, with quantum efficiencies of 0.32 and 0.25, respectively.[53] Both of these probes exhibit relatively high pK_a values for the benzylic nitrogen atoms, 8.4 for ZP1 and 9.4 for ZP2, which indicates that the nitrogen atoms responsible for PET quenching are protonated at physiological pH and unable to quench the fluorophore excited state effectively. In an attempt to lower the background fluorescence of the free ZP dyes, ZP4 was developed and incorporates an aniline-type nitrogen as the donor since it has a lower pK_a value than aliphatic nitrogen atoms. ZP4 exhibits relatively low background fluorescence ($\phi = 0.06$) at pH 7, and the aniline-type nitrogen atom has a pK_a of 7.2. With this relationship in mind, the syntheses of the ZP4 analogues ZP5, ZP6, and ZP7 were undertaken to determine whether substitution in the para position would influence the aniline nitrogen atom pK_a and background fluorescence of the sensor. A comparison of the physical properties obtained for the unsymmetrical ZP4 analogues reveals both expected and unexpected behavior.

The physical characteristics of ZP4 are documented elsewhere.[54] ZP5, ZP6, and ZP7 show changes in their optical spectra that are similar to those of ZP4 upon binding Zn(II). All four probes display a ~10 nm blue shift upon addition of Zn(II), which indicates perturbation of the fluorescein π-system caused by coordination of the Zn(II) to the phenol oxygen atom. The difference spectrum for each probe reveals that the addition of Zn(II) is accompanied by increases in absorption at 462 nm and ~491 nm and decreases at 512 nm. Both Job plot analyses and metal-binding titrations suggest formation of a 1:1 complex for each sensor, which has been supported crystallographically through the study of several model complexes.[54] The K_d values for ZP4, ZP5, and ZP6 are all in the sub-nanomolar range. Although the K_d of ZP7 was not determined since its fluorescence change is negligible upon addition of Zn(II), we can assume that it binds Zn(II) with comparable affinity. Like ZP4, ZP5 and ZP6 are selective sensors for Zn(II) and Cd(II), and the Zn(II)-induced fluorescence is not compromised in a background of Ca(II), Mg(II), and Mn(II). In the presence of other divalent first-row transition metals such as Fe(II), Co(II), Ni(II), and Cu(II), no fluorescence change is observed upon addition of Zn(II) for ZP4, ZP5, and ZP6. These similarities are not surprising because the sensors utilize the same fluorophore and metal-binding motif.

Unlike the properties described above, a comparison of the fluorescence enhancement upon Zn(II) binding, quantum efficiencies, and protonation constants of the unsymmetrical ZP sensors reveals some unexpected behavior. Each unbound probe has an emission maximum ~520 nm that blue-shifts by ~5 nm upon Zn(II) binding. Since aniline nitrogen atoms have low affinity for protons, it was anticipated that each of the unsymmetrical probes would exhibit a low quantum yield, relative to those of ZP1 and ZP2, at physiological pH in the metal-free form. Such expected behavior was observed for unbound ZP4, as previously shown,[54] and for unbound ZP6 and ZP7. In contrast, the quantum efficiency for free ZP5 is relatively high, 0.29, and comparable to that observed for ZP1 (0.38) and ZP2 (0.29), symmetrical species that do not contain an aniline-type nitrogen atom linking the ligand fragment to the fluorophore. These variations in quantum efficiency can be correlated to the pK_a values for the nitrogen atoms that participate in PET. The pK_a for the aniline nitrogen atom in ZP4 is 7.2, indicating that it is deprotonated at physiological pH and resulting in effective PET quenching. ZP6 and ZP7 also exhibit relatively low pK_a values for the aniline nitrogen atoms, 6.3 and 6.9, respectively. In contrast, the aniline nitrogen atom of ZP5 has a pK_a of 9.6, a value similar to those observed for ZP1 (8.4) and ZP2 (9.4), which presumably inhibits PET quenching and causes its relatively high background fluorescence. The origin of the high pK_a value for ZP5 remains unclear.

The fluorescence behavior of ZP7 is also anomalous. Only negligible fluorescence enhancement occurs upon Zn(II) coordination. The methoxy substituent clearly causes this effect, but the mechanism is not understood. A secondary quenching mechanism, perhaps involving the methoxyether oxygen atom, is one possible explanation.

Cell Permeability Studies of ZP Dyes. The first-generation ZP dyes, ZP1 and ZP2, are intracellular Zn(II) sensors that diffuse passively across the cell membrane.[53] These sensors resemble the cell-permeable heavy metal ion chelator *N*′,*N*′,*N*″,*N*″-tetra(2-picolyl)ethylenediamine (TPEN) and are charge-neutral at physiological pH. In contrast, ZP4 is cell impermeable. Since ZP4 contains an aniline-type nitrogen atom with a pK_a of 7.2, it was postulated that the overall charge of −1 might be responsible for its impermeability.[54] Like ZP4, ZP6 carries a charge of −1 at physiological pH and is unable to cross the cell membrane. Due to its pK_a of 9.6, the aniline nitrogen atom of ZP5 is protonated at pH 7, resulting in an unsymmetrical probe with no charge. After incubating HeLa cells at 37 °C with ZP4, ZP5, or ZP6 and subsequently treating them with Zn-pyrithione, no staining whatsoever was observed (data not shown). ZP1 was used as a positive control. These cell permeability studies indicate that, regardless of the overall charge, asymmetrical ZP4-like sensors cannot diffuse passively across the cell membrane. Some other factor(s), such as ligand properties or the ability of the fluorescein to adopt the lactone isomer, must be more important than overall charge in determining cell permeability.

(59) Nolan, E. M.; Chang, C. J.; Lippard, S. J. Unpublished results.

Summary. A new unsymmetrical fluorescein platform, **16**, has been developed and its utility demonstrated in the assembly of several ZP sensors. The aldehyde functionality in the 4′ position is well suited for the assembly of ZP probes or other metal ion sensors that incorporate an aniline nitrogen atom as the PET quenching unit. Three new unsymmetrical ZP sensors based on ZP4 have been synthesized and characterized in order to determine the effects of various substituents (X = H, F, Cl, OMe) para to the aniline nitrogen atom on the electronic properties of the sensor. These sensors exhibit both expected and unexpected behavior. The data illustrate the predictability of relative background fluorescence based on the pK_a of the aniline nitrogen atom. A comparison of the photophysical properties for free and Zn(II)-bound ZP4−7 reveals that the details of their fluorescence behavior are complex and cannot be predicted through consideration of substituent effects alone.

Acknowledgment. This work was supported by Grant GM65519 from the National Institute of General Medical Sciences. NIH Grant 1S10RR13886-01 and NSF Grants CHE-9808063, DBI9729592, and CHE-9808061 were used to maintain spectroscopic equipment. E.M.N. thanks NDSEG for a graduate fellowship and Olga Burenkova and Katie R. Barnes for assistance with the cell permeability studies.

Supporting Information Available: Figures S1−3. This material is available free of charge via the Internet at http://pubs.acs.org.

IC035158+